A Millimeter-shaped Metal-Organic Framework/Inorganic Nanoparticle Composite as a New Adsorbent for Home Water-Purification Filters

Gerard Boix[†], Xu Han[†], Inhar Imaz[†]* and Daniel Maspoch[†‡]*

[†]Catalan Institute of Nanoscience and Nanotechnology (ICN2), CSIC and The Barcelona Institute of Science and Technology, Campus UAB, Bellaterra, 08193, Barcelona, Spain

[‡]ICREA, Pg. Lluis Companys 23, 08010, Barcelona, Spain

Keywords: Metal-Organic Frameworks, Composites, Inorganic Nanoparticles, Metal removal, Water treatment and purification

ABSTRACT: Heavy-metal contamination of water is a global problem with an especially severe impact in countries with old or poorly-maintained infrastructure for potable water. An increasingly popular solution for ensuring clean and safe drinking water in homes is the use of adsorption-based water filters, given their affordability, efficacy and simplicity. Herein, we report the preparation and functional validation of a new adsorbent for home water-filters, based on our composite of the metal-organic framework (MOF) UiO-66 and cerium (IV) oxide (CeO_2) nanoparticles. We began by preparing UiO-66@CeO_2 microbeads, and then encapsulating them into porous polyethersulfone (PES) granules, to obtain millimeter-scale CeO_2@UiO-66@PES granules. Next, we validated these granules as an adsorbent for removal of metals from water, by substituting them for the standard absorbent (ion-exchange resin spheres) inside a commercially available water pitcher from Brita®. We assessed their performance according to the American National Standards Institute (ANSI) guideline 53-2019, "Drinking Water Treatment Units - Health Effects Standard". Remarkably, a pitcher loaded with a combination of our CeO_2@UiO-66@PES granules and activated carbon at standard ratios met the target reduction thresholds set by NSF/ANSI 53-2019 for all the metals tested: As(III), As(V), Cd(II), Cr(III), Cr(VI), Cu(II), Hg(II) and Pb(II). Throughout the test, the modified pitcher proved to be robust and stable. We are confident that our findings will bring MOF-based adsorbents one step closer to real-world use.

1. INTRODUCTION

According to the United Nations, millions of people die annually from diseases associated with inadequate water supply, sanitation and hygiene, with children being particularly affected.[1] Much of this is due to drinking water contaminated with heavy metals, which, even at trace levels, pose considerable health risks.[2–4] Accordingly, as part of its seventeen sustainable development goals, the United Nations has stipulated that "safe water and adequate sanitation are indispensable for healthy ecosystems, reducing poverty, and achieving inclusive growth, social well-being and sustainable livelihoods".[5] Therefore, there is a pressing need to develop strategies and products to provide clean water. Water-remediation processes are usually performed at the source, in industrial treatment plants that employ large-scale processes such as coagulation, filtration and chemical precipitation.[6] However, these large-scale treatments have difficulties reducing pollutants at low concentrations and generate large quantities of sub-products like sludge,[7] meaning that additional purification processes are usually required.

Supplementary water-purification treatments can be performed directly by consumers at home by using water filters mounted in or on refrigerators, faucets, plumbing, squeeze bottles; or when traveling, by using portable units. Most current domestic water-remediation systems rely on either reverse-osmosis or

adsorption. Although reverse-osmosis systems can remove nearly all the dissolved solids from a water stream, they tend to be slow, expensive and wasteful, making them less attractive for developing regions. Adsorption systems are usually cheaper; however, the common adsorbents (*e.g*. activated carbon, zeolites or natural fibers) exhibit low capacity, costly regeneration and poor selectivity, especially to harmful contaminants (*e.g.* arsenic) that are typically present in higher concentrations in developing regions than in more developed areas.[8,9] Thus, most adsorption-based filters, including the well-known pour-through type pitcher products, employ a combination of several materials with complementary adsorption profiles. The most common combination is that of an ion-exchange resin, to remove dangerous heavy metals, with activated carbon, to remove organic substances that compromise the taste and odor of drinking water.[10]

Researchers have endeavored to find alternative materials for water remediation that exhibit superior adsorption kinetics, capacity and/or regeneration compared to the state of the art. Amongst the most promising candidates are porous materials such as metal organic frameworks (MOFs) and covalent organic frameworks (COFs), which offer large surface areas and the possibility of being chemically tuned. In fact, MOFs and COFs have already demonstrated their efficacy at water remediation,[11–19] even under continuous flow conditions.[20-22] This is the case of MOFs such as the MIL, ZIF and UiO families, which excel at metal removal.[23–30] Nonetheless, the widespread adoption of MOFs into real-world use still faces several hurdles.[16,30,31] These include challenges in the processability of MOFs, in shaping them from nano- or micro-scale powders to macroscale objects, and in validating them in studies focused on development of an actual product. For example, there has been a lack of studies on MOF-based materials in the testing conditions stipulated in nationally recognized standards for evaluating and certifying water-purification systems. Thus, most of the literature on adsorption of pollutants from water by MOFs encompasses studies performed under the narrowly controlled conditions necessary for obtaining reliable experimental data, which in turn cannot always be directly extrapolated to real-life conditions.[32]

Our group previously reported microbeads of the composite CeO_2@UiO-66, comprising the metal-organic framework (MOF) UiO-66 and cerium (IV) oxide (CeO_2) nanoparticles, for use in water purification.[33] This composite offers a complementary adsorption profile that draws on the functionality of each component. Particularly, UiO-66 provides a high surface area, water stable substrate where different metals can bind. According to previous studies,[34-36] the kinetics of metal ion adsorptions in UiO-66 frameworks is governed by a pseudo-second order model, implying chemisorption as the main driving force. The most probable binding sites are located at defects on the framework; as, for example, on the SBUs in which open metal sites of the zirconium clusters can interact with anionic oxyanions like Cr(VI) and As(V).[36] Despite the non-specific broad adsorption capabilities of UiO-66 for metals, its affinity for As(III) ions is however very low.[33] Thus, the incorporation of CeO_2 nanoparticles into MOF microbeads enhances adsorption of As(III) (and also of Cr(VI)) thanks to their previously reported activity and selectivity towards both metals.[37,38] Importantly, the CeO_2@UiO-66 microbeads can be synthetized through a scalable, continuous-flow spray-drying methodology and can be regenerated. Here, we report on testing of this composite for removal of metals from water in a commercially available filter pitcher, which we assessed by replacing the standard adsorbent in the filter with our composite, under U.S. government guidelines. Adsorbents used in home water-filter pitchers are usually shaped at the macroscale to facilitate their handling and to avoid the toxicity associated with manipulating powders. Accordingly, we first shaped our CeO_2@UiO-66 microbeads by encapsulating them into porous, millimeter-sized polyethersulfone (PES) granules to create CeO_2@UiO-66@PES granules. We chose PES because it is a commonly used polymer in water-

remediation filters such as ultrafiltration membranes and reverse-osmosis devices.[39–41] Next, following the American National Standards Institute (ANSI) guideline 53-2019, "Drinking Water Treatment Units - Health Effects Standard",[42] we evaluated the performance of CeO_2@UiO-66@PES granules at removing metals from water within a commercial water filter pitcher from Brita®. To this end, we replaced the adsorbent of the stock Brita® filter, ion-exchange resin spheres, with our CeO_2@UiO-66@PES granules, either alone or in combination with the same activated carbon provided in stock default filter, which is used to adsorb organics that affect the taste and odor of water. We then compared our modified filters to the stock one for metal removal. Remarkably, we first demonstrated that MOF-based granules can meet the target reduction thresholds set by NSF/ANSI 53-2019 for all the metals tested: As(III), As(V), Cd(II), Cr(III), Cr(VI), Cu(II), Hg(II) and Pb(II).

2. MATERIALS AND METHODS

2.1. Materials. Zirconium (IV) propoxide solution (70% (w/w)) in 1-propanol; cerium (III) nitrate; sodium meta arsenite; sodium arsenate dibasic heptahydrate; cadmium (II) chloride; chromium (III) chloride hexahydrate; potassium dichromate; copper (II) sulfate; lead (II) nitrate; mercury (II) chloride; terephthalic acid; sodium metasilicate; sodium bicarbonate; magnesium sulfate; sodium nitrate; sodium fluoride; sodium dihydrogen phosphate; sodium hydroxide; calcium chloride; sodium hypochlorite and polyvinylpyrrolidone (PVP; M_w ~ 10,000) were purchased from Sigma Aldrich. *N,N*-dimethylformamide; methanol; hydrochloric acid and acetone were purchased from Fisher Scientific. All the reagents were used without further purification. Deionized water, obtained with a Milli-Q® system (18.2 MΩ cm), was used in all adsorption experiments. X-ray powder diffraction (XRPD) patterns were collected on an X'Pert PRO MPDP analytical diffractometer (Panalytical) at 45 kV and 40 mA using CuKα radiation (λ = 1.5419 Å). Nitrogen adsorption and desorption measurements were collected at 77 K using an ASAP 2460 (Micromeritics). Temperature for N_2 isotherms measurement was controlled by using a liquid nitrogen bath. FE-SEM images were collected on a Magellan 400 L scanning electron microscope (FEI) at an acceleration voltage of 5.0 KV. Transmission electron microscopy (TEM) images were collected on a Tecnai G2 F20 microscope (FEI) at 200 KV. ^{1}H NMR spectra were acquired in a Bruker Avance III 400SB NMR spectrometer. Inductively Coupled Plasma – Optical Emission Spectroscopy (ICP-OES) measurements were performed on an Optima 4300DV (Perkin-Elmer) instrument. ICP-MS were performed on an Agilent 7500. All Hg ions were analyzed on a Direct mercury analyzer DMA-80 (Milestone).

2.2. Synthesis of PVP-functionalized CeO_2 nanoparticles. The CeO_2 nanoparticles were synthesized according to modified published procedures.[43,44] In a typical experiment, equal volumes of aqueous $Ce(NO_3)_3$ (75 mL, 0.04 M) and aqueous hexamethylenetetramine (75 mL, 0.50 M) were mixed at room temperature, and the resultant solution was left at 25 °C for 48 hours under mild stirring. CeO_2 nanoparticles were formed by the controlled oxidation of Ce(III) to Ce(IV) under alkaline conditions, which subsequently precipitated in the form of insoluble CeO_2 species. A solution of 4 g of PVP in 200 mL of water was added dropwise to a stirring solution of the CeO_2 nanoparticles, and the flask was left to rest overnight at room temperature. Then, 800 mL of acetone was added, and the solution was left at room temperature for 24 hours without stirring, leading to precipitation of the nanoparticles. The supernatant was removed by decanting, and then the nanoparticles were washed three times with DMF. Finally, they were redispersed in DMF to afford a colloidal solution of CeO_2 nanoparticles (1 mg mL^{-1}). The average size of the synthesized CeO_2 nanoparticles was 12 nm ± 2.5 nm.

2.3. Synthesis of CeO_2@UiO-66 microbeads. CeO_2@UiO-66 microbeads were synthesized using our previously reported spray-drying method.[33,45] Briefly, terephthalic acid (0.6 mmol, 100 mg), glacial acetic acid (3 mL), a solution of CeO_2 nanoparticles in DMF (7 mg mL^{-1}; 2 mL) and a 70% (w/w) solution of zirconium (IV) propoxide ($Zr(OPr^n)_4$) in 1-propanol (0.5 mmol, 280 µL) were sequentially added to a flask containing 40 mL of DMF. The resulting mixture was injected into a coil-flow reactor (inner diameter: 3 mm) at a feed rate of 2.4 mL min^{-1} at 115 ˚C. The resulting pre-heated solution was then spray-dried at 180 ˚C, at a flow rate of 336 mL min^{-1}, using a B-290 Mini Spray-Dryer (BUCHI Labortechnik; spray cap hole diameter: 0.5 mm). The resulting solid was dispersed in DMF, washed twice with DMF and ethanol, and finally, dried for 12 h at 85 °C under vacuum. The encapsulation efficiency of CeO_2 nanoparticles was determined by ICP-OES and was found to be 4.3% w/w (93% encapsulation yield).

2.4. Synthesis of CeO_2@UiO-66@PES granules. The CeO_2@UiO-66@PES granules were shaped via a modified phase-inversion synthesis adapted from the literature.[46] Briefly, a homogeneous dispersion containing 4.5 g of CeO_2@UiO-66 microbeads and 15 g of PES dissolved in 100 mL of DMF (30 % of microbeads (w/w) in relation to PES in the solution) was prepared. The mixture was left stirring at high rpm for 1 hour to assure homogeneous distribution of the microbeads throughout the PES solution. In parallel, 800 mL of a water/ethanol mixture (1:1) was prepared and cooled down to 0ºC in an ice bath. The CeO_2@UiO-66 microbeads-PES dispersion was then added dropwise to the chilled water-ethanol solution under mild stirring. As the droplets of this dispersion enter in contact with the water/ethanol bath, the PES instantly precipitated forming the granules. The formed granules were left stirring for 1 hour in the same bath to slowly diffuse the DMF trapped inside, resulting in a hard, sponge-like granular structure. The water/ethanol bath was replaced with a fresh one a couple of times to properly clean the formed granules. Afterwards, they were left overnight stirring to evacuate all DMF that could still remain inside the porous structure. Finally, they were decanted out, left in the open air to dry and stored until use. The obtained material was characterized by XRPD (Figure 1e), FE-SEM (Figure 1d) and N_2 sorption (Figure 1f). The synthesis was repeated with 7% or 60% CeO_2@UiO-66 microbeads (w/w) relative to the PES in solution. The exact amount of microbeads inside the granules was measured by analyzing the contents of Zr(IV) and Ce(IV) ions of digested samples of the granules by ICP-MS. Loading values of 6.7%, 26.1%, and 47.4% (w/w) of CeO_2@UiO-66 microbeads were found, which translate to encapsulation efficiency values of 90%, 87% and 79% for the samples synthesized using 7%, 30% and 60% (w/w) CeO_2@UiO-66 microbeads relative to the PES in solution, respectively. For the 0% loading granule sample, the granule synthesis experiment was repeated with a pristine 0.15 g mL^{-1} PES solution.

2.5. Heavy metal contaminated water preparation. Water samples were prepared according to the specifications described in the NSF/ANSI 53-2019 standard. Briefly, artificial ¨hard¨ tap water was prepared by dissolving 279 mg of Na_2SiO_3, 750 mg $NaHCO_3$, 344 mg $MgSO_4$, 36 mg $NaNO_3$, 6.6 mg NaF, 0.5 mg $NaH_2PO_4{\cdot}H_2O$, 333 mg $CaCl_2$ and 1.5 mg NaClO into 3 L mili-Q water. The pH of the water was corrected to 6.5 or 8.5 using HCl/NaOH, and the water was then stored in the dark until use. To prepare the metal pollutant solutions, 4.3 mg of $NaAsO_2$, 6.9 mg of Na_2HAsO_4, 4.1 mg $CdCl_2$, 12.8 mg $CrCl_3{\cdot}6H_2O$, 14.3 mg $Na_2Cr_2O_7{\cdot}2H_2O$, 9.8 mg $CuSO_4{\cdot}5H_2O$ and 4.3 mg $Hg(NO_3)_2{\cdot}H_2O$ were dissolved into 250 mL mili-Q water acidified to pH 1 to produce solutions of each metal ion at 10 ppm. To avoid precipitation, the Pb solution was prepared by dissolving 3.6 mg of $Pb(NO_3)$ into 4 mL of a 1:1 mixture of mili-Q water and concentrated HNO_3, resulting in a 563.4 ppm Pb solution. An initial sample of contaminated with heavy metal ions (100 ppb each of As(III), As(V), Cd(II), Cr(III), Cr(VI), Cu(II), Hg(II) and Pb(II)) was prepared by dissolving the stock metal solutions in 3 L synthetic “hard” water. Also, to meet the specified concentrations dictated by the

NSF/ANSI 53-2019, eight contaminated water samples were prepared, each of which contained 50 ppb As(III); 50 ppb As(V); 30 ppb Cd(II); 300 ppb Cr(III); 300 ppb Cr(VI); 1200 ppb Cu(II); 6 ppb Hg(II); and 150 ppb Pb(II). To this end, the prepared stock metal solutions were dissolved in 3 L synthetic "hard" water each. The pH of the as-prepared solutions was checked for excessive drifting and corrected with HCl/NaOH if necessary. The solutions were stored at 4 ˚C in the dark until use.

2.6. Continuous-flow metal capture experiments. To determine the optimum loading of CeO_2@UiO-66 microbeads into the polymeric granules for effective metal capture, four samples of CeO_2@UiO-66@PES granules containing 0%, 6.7%, 26.1% or 47.4% (w/w) of CeO_2@UiO-66 microbeads were synthetized. Briefly, 0.3 g of each granule were loaded into an HPLC column (diameter = 1 cm) connected to a peristaltic pump (Figure S4). The water solution containing 100 ppb each of As(III), As(V), Cd(II), Cr(III), Cr(VI), Cu(II), Hg(II) and Pb(II) ions was filtered through the column at a flow-rate of 0.5 ml min^{-1}, and the filtrate was collected, and then analyzed by ICP.

2.7. Cartridge metal capture experiments. Metal capture experiments were performed using either a commercial Brita® cartridge or a modified cartridge filled with activated carbon (53 g) only, with CeO_2@UiO-66@PES granules (18 gr) only, or with a mixture of activated carbon (35 g) and CeO_2@UiO-66@PES granules (18 g). For each pollutant, 1 L of heavy metal-contaminated water (at the concentrations specified in NSF/ANSI 53-2019) was filtered through the pitcher, and then collected for ICP analysis. For comparison purposes, all experiments were repeated with a modified cartridge containing only CeO_2@UiO-66@PES granules and a pristine Brita® cartridge filter.

3. RESULTS AND DISCUSSION

3.1. Synthesis and characterization. First, we synthesized CeO_2@UiO-66 microbeads by the continuous-flow spray-drying methodology that our group previously reported.[33,45] In a typical synthesis, a *N,N*-dimethylformamide (DMF) solution of terephthalic acid (15 mM), acetic acid (1.3 M), zirconium propoxide solution in propanol (70%) (15 mM) and dispersed CeO_2 nanoparticles (350 mg L^{-1}) was injected into a coil-flow reactor, and then spray-dried, leading to formation of spherical microbeads (average size: 2.5 µm ± 2.0 µm) comprising nanocrystals of UiO-66 (average size: 20 nm) and CeO_2 nanoparticles (4.5% in weight) homogeneously dispersed throughout (Figure 1a,b). N_2-sorption analysis at 77 K revealed a BET surface area of 1017 m^2 g^{-1} (Figure S1). As we expected for this type of microbead synthesized by spray-drying, we found the collected isotherm to be a type-IV (IUPAC classification) isotherm that features a hysteresis loop. We attributed this behavior to the presence of some mesoporosity resulting from the assembly of the UiO-66 nanocrystals in the microbeads.[47]

- Figure 1 -

Shaping of MOF-based powders is crucial for decreasing the health hazards related to the manipulation of fine powders as well as for facilitating their handling and their integration into devices. Thus, we shaped CeO_2@UiO-66 microbeads at the macroscale by immobilizing them into millimeter-scale (size = 1.9 mm to 2.1 mm), porous polymeric PES granules (Figure 1c,d), to obtain CeO_2@UiO-66@PES granule that ultimately resembled the ion-exchange resin spheres typically employed in home water filters. This process began with preparation of 100 mL of a solution containing PES in DMF (150 mg mL^{-1}), into which the CeO_2@UiO-66 microbeads were then dispersed (final microbeads concentration of 45 mg mL^{-1}, 30%

w/w with PES). The resultant dispersion was poured dropwise onto a 1:1 mixture of water/ethanol pre-cooled to 0 ˚C. The PES instantly precipitated, forming a hard shell around the droplets, which were left stirring in the precipitation bath for 3 h to allow the DMF trapped inside to slowly diffuse, thereby enabling formation of the porous channels inside the droplets. The precipitation bath was renewed with fresh H_2O/ethanol (1:1) and left stirring for additional 3 h. Next, the DMF-free granules were collected by decantation of the liquid, and then redispersed in pure ethanol overnight. Finally, the resultant clean granules were dried under dynamic vacuum at 85 ˚C and stored until use.

Field-emission scanning electron microscopy (FE-SEM) of the cross-sections of CeO_2@UiO-66@PES granules revealed their macroporous nature and that CeO_2@UiO-66 microbeads were indeed dispersed throughout the inner surface of the granule (Figures 1e,f). In these granules, interaction between microbeads and PES is mainly attributed to "π-π" interactions between the phenylene groups of UiO-66 and the polyethersulfone backbone.[48] Moreover, X-ray powder diffraction (XRPD) analysis of the granules confirmed that the crystallinity of CeO_2@UiO-66 microbeads had not been affected (Figure 2a). Samples of CeO_2@UiO-66@PES granules were digested in 5% HF and 70% HNO_3, and then analyzed for Zr and Ce ions by inductively-coupled plasma-mass spectrometry (ICP-MS) to confirm the loading of microbeads inside the granules, which was found to be 26.1%. N_2-sorption analysis at 77 K revealed a BET surface area of 260 $m^2\ g^{-1}$ (Figure 2b, Figure S2), which is close to the expected value (265 $m^2\ g^{-1}$) according to the loading percentage of CeO_2@UiO-66 within the granules. This result demonstrated that encapsulation of the CeO_2@UiO-66 microbeads inside the PES granules does not compromise their sorption capacity.

- Figure 2 -

Shaping of MOF-based powders is crucial for decreasing the health hazards related to the manipulation of fine powders as well as for facilitating their handling and their integration into devices. Thus, we shaped CeO_2@UiO-66 microbeads at the macroscale by immobilizing them into millimeter-scale (size = 1.9 mm to 2.1 mm), porous polymeric PES granules (Figure 1c,d), to obtain CeO_2@UiO-66@PES granule that ultimately resembled the ion-exchange resin spheres typically employed in home water filters. This process began with preparation of 100 mL of a solution containing PES in DMF (150 mg mL^{-1}), into which the CeO_2@UiO-66 microbeads were then dispersed (final microbeads concentration of 45 mg mL^{-1}, 30% w/w with PES). The resultant dispersion was poured dropwise onto a 1:1 mixture of water/ethanol pre-cooled to 0 ˚C. The PES instantly precipitated, forming a hard shell around the droplets, which were left stirring in the precipitation bath for 3 h to allow the DMF trapped inside to slowly diffuse, thereby enabling formation of the porous channels inside the droplets. The precipitation bath was renewed with fresh H_2O/ethanol (1:1) and left stirring for additional 3 h. Next, the DMF-free granules were collected by decantation of the liquid, and then redispersed in pure ethanol overnight. Finally, the resultant clean granules were dried under dynamic vacuum at 85 ˚C and stored until use.

Field-emission scanning electron microscopy (FE-SEM) of the cross-sections of CeO_2@UiO-66@PES granules revealed their macroporous nature and that CeO_2@UiO-66 microbeads were indeed dispersed throughout the inner surface of the granule (Figures 1e,f). In these granules, interaction between microbeads and PES is mainly attributed to "π-π" interactions between the phenylene groups of UiO-66 and the polyethersulfone backbone.[48] Moreover, X-ray powder diffraction (XRPD) analysis of the granules confirmed that the crystallinity of CeO_2@UiO-66 microbeads had not been affected (Figure 2a). Samples of CeO_2@UiO-66@PES granules were digested in 5% HF and 70% HNO_3, and then analyzed for Zr and Ce ions by inductively-coupled plasma-mass spectrometry (ICP-MS) to confirm the loading of microbeads

inside the granules, which was found to be 26.1%. N_2-sorption analysis at 77 K revealed a BET surface area of 260 m^2 g^{-1} (Figure 2b, Figure S2), which is close to the expected value (265 m^2 g^{-1}) according to the loading percentage of CeO_2@UiO-66 within the granules. This result demonstrated that encapsulation of the CeO_2@UiO-66 microbeads inside the PES granules does not compromise their sorption capacity.

- Figure 3 -

3.3. CeO_2@UiO-66@PES granules as a metal adsorbent in home water-filter pitchers. As our main objective was to evaluate a MOF-based adsorbent for home water-purification under real-world conditions, we assessed the performance of our CeO_2@UiO-66@PES granules as a replacement adsorbent within a commercially available water-filter pitcher from Brita® (Figure 4a). Such pitchers are equipped with a filter cartridge that contains a mixture of activated carbon, to remove organics that affect the taste and odor of water, and ion-exchange resin spheres, to remove heavy metals. The stock cartridge provided with the Brita® model that we chose contains ~35 g activated carbon and ~18 g ion-exchange resin spheres.

Beyond wanting to test our CeO_2@UiO-66@PES granules inside the cartridge of a real filter pitcher under real-world conditions, we also wanted to assess the performance according to existing regulations on commercialization of products that are claimed to remove harmful substances. In the United States, this is covered by guideline NSF/ANSI 53-2019, "Drinking Water Treatment Units - Health Effects Standard", of the American National Standards Institute (ANSI). This guideline establishes the minimum performance requirements for point-of-use and point-of-entry drinking water systems (*e.g.* refrigerator filters; plumbed-in systems; and non-plumbed, pour-through-type batch treatment systems such as filter pitchers), which are designed to reduce specific health-related contaminants from public or private water supplies.

Accordingly, we assayed our CeO_2@UiO-66@PES granules as a potential adsorbent of metal contaminants in modified cartridges within a Brita® pitcher, according to guideline NSF/ANSI 53-2019. To this end, we first emptied out the filter cartridge of its default adsorbents. Then, we refilled it with either CeO_2@UiO-66@PES granules (18 g) alone, or with a mixture of activated carbon (35 g) and CeO_2@UiO-66@PES granules (18 g) (Figure 4b). The cartridge containing the CeO_2@UiO-66@PES granules alone served to determine their performance at removing metal contaminants in the absence of a second adsorbent, whereas the cartridge containing the mixture (granules + activated carbon) served to mimic the composition of the stock cartridge. As controls, the standard Brita® cartridge, and a modified one containing only activated carbon (53 g), were also used.

We then separately tested each of the four cartridges in the same Brita® **(**Figure 4a**)**. As per the specifications of the NSF/ANSI 53-2019 standard, 1 L of each solution containing a metal pollutant [As(III), As(V), Cd(II), Cr(III), Cr(VI), Cu(II), Hg(II) and Pb(II)] was then filtered through the pitcher, and an aliquot of the resulting filtrate for each solution was collected for analysis by ICP-MS. Note that the sixteen liters (each one corresponding to a different metal ion, at two different pH values) were consecutively filtered through each cartridge, without any change of the corresponding filler material. Each heavy-metal solution was prepared using synthetic hard water (pH 6.5 or pH 8.5) containing the following inorganic salts: 93 ppm $Na_2SiO_3 \cdot 9H_2O$; 250 ppm $NaHCO_3$; 128 ppm $MgSO_4 \cdot 7H_2O$; 12 ppm $NaNO_3$; 2.2 ppm NaF; 0.18 ppm $NaH_2PO_4 \cdot H_2O$; 111 ppm $CaCl_2$; and 1 ppm NaClO. Again, per the NSF/ANSI 53-2019 standard

instructions, the concentration of metal ions in this solution was specified to be 50 ± 10 ppb As; 30 ± 7 ppb Cd; 300 ± 75 ppb Cr; 3000 ± 750 ppb Cu; 6 ± 1 ppb Hg; and 150 ± 15 ppb Pb.

- Figure 4 -

Table 1 shows the target influent solution concentration, the measured influent solution concentration, the reduction target concentration (per NSF/ANSI 53-2019) and the effluent concentration, with the corresponding adsorption values (percentage) for each cartridge. As expected, the cartridge containing only activated carbon exhibited the worst performance overall (Table 1, Figure 4c), barely removing any of the metal ions, except for Cu(II) (86% to 88%) and Pb(II) (64% to 73%) at both pH 6.5 and pH 8.5. Thus, the effluent concentration only met the target reduction set by the NSF/ANSI 53-2019 standard for Cu(II) ions at both pH 6.5 and pH 8.5. Contrariwise, the pitcher loaded with the standard Brita® filter cartridge performed very well, meeting the requirements for all metal ions, except for As(III) and As(V), at both pH 6.5 and pH 8.5.

The cartridge loaded with CeO_2@UiO-66@PES granules reduced the influent concentration of the metal pollutants to (values at pH 6.5 and at pH 8.5): 12 ppb and 10 ppb As(III); 10 ppb and 9 ppb As(V); 2 ppb and 3 ppb Cd(II); 73 ppb and 74 ppb Cr(III); 97 ppb and 91 ppb Cr(VI); 701 ppb and 652 ppb Cu(II); 1.4 ppb and 1.5 ppb Hg(II); and 5 ppb and 4 ppb Pb(II). Thus, at both pH values, it reduced the effluent concentration of each metal ion to below the requirement of the NSF/ANSI 53-2019, except for As(III) at pH 6.5. These results corroborate the efficacy of CeO_2@UiO-66 microbeads at removing metal pollutants, even when they are immobilized within a polymeric matrix.

The cartridge containing the mixture of CeO_2@UiO-66@PES granules and activated carbon was even more effective, as it reduced the effluent concentration of each metal ion to below the requirement of the NSF/ANSI 53-2019 standard, to (values at pH 6.5 and at pH 8.5): 10 ppb and 9 ppb As(III); 9 ppb and 8 ppb As(V); 1 and 2 ppb Cd(II); 60 ppb and 41 ppb Cr(III); 75 ppb and 82 ppb Cr(VI); 151 ppb and 250 ppb Cu(II); 1.0 ppb and 1.0 ppb Hg(II); and 1 ppb and 1 ppb Pb(II). This reduction confirms that, when the standard ion-exchange spheres of the filter cartridge are replaced with the same mass of CeO_2@UiO-66@PES granules, the resultant cartridge fulfils the minimum performance requirements for removal of various metals from water, including As(III) and As(V), which were not efficiently adsorbed by the stock cartridge, in point-of-use or point-of-entry potable-water systems. Note that these results are even more remarkable if one considers that only 26.1% (4.7 g) of the 18 g of granules loaded into the cartridge corresponds to active CeO_2@UiO-66 microbeads, corresponding to 4.5 g of UiO-66 and 0.2 g of CeO_2 nanoparticles.

- Table 1 -

Having demonstrated the efficacy of our CeO_2@UiO-66@PES granules in single-use experiments, we next sought to ascertain their performance over repeated use. To this end, we tested the same cartridge containing our CeO_2@UiO-66@PES granules and activated carbon that we used in the previous filtration experiments, for its capacity to remove As(III) from an additional 16 L of synthetic “hard” water containing 50 ppb As(III), at pH 6.5. ICP-MS analysis of each liter of the filtered water revealed similar adsorption rates for each of the additional 16 L, thereby indicating that the CeO_2@UiO-66@PES granules within the cartridge had fully retained their adsorption capacity (Figure 5).

Finally, given that the adsorbents used in water purification must not pollute the water themselves, we sought the assess the stability of our CeO_2@UiO-66@PES granules by confirming that they do not release their constituent metal ions of Zr(IV) and Ce(IV) into water. Accordingly, we also investigated the presence of these metal ions in the aqueous solutions in all the adsorption experiments done throughout this study. Importantly, we did not detect any Zr(IV) or Ce(IV) in any of the filtered water samples, thus confirming the stability of the microbeads. Also, N_2-sorption analysis at 77 K of the granules after the filtration experiments and regenerated by washing with a 250 mM aqueous solution of $H_2PO_4^-$ (pH 5)[33] revealed a BET surface area of 240 $m^2 g^{-1}$ (Figure S7),[49] which is very close to their initial value (260 $m^2 g^{-1}$). Moreover, XRPD performed on the granules and their general aspect and morphology after the filtration experiments suggest that they had not been affected at any point during testing (Figures S7, S8).

- Figure 5 -

4. CONCLUSION

We have developed and validated a MOF-based composite for removal of metal pollutants from drinking water, which is amenable to use in the cartridges in home filter pitchers. We first prepared microbeads of the composite, which comprises the MOF UiO-66 and CeO_2 nanoparticles, via one-step, continuous-flow spray-drying synthesis, and then encapsulated them into PES granules to obtain millimeter-size CeO_2@UiO-66@PES granules. We next assayed these granules for adsorption of metals from water under real-world conditions, including as a replacement adsorbent in the cartridge of a commercially available pitcher, according to US government guidelines (NSF/ANSI 53-2019) for home water purification. A cartridge containing a combination of our CeO_2@UiO-66@PES granules and activated carbon, in the same ratio as the ion-exchange resin and activated carbon used in the stock cartridge, met the NSF/ANSI 53-2019 purification requirements for removal of As(III), As(V), Cd(II), Cr(III), Cr(VI), Cu(II), Hg(II) and Pb(II) from water at two different pH levels. This result is especially impressive, given that the stock cartridge provided with the filter pitcher could not meet these requirements for As(III) or As(V). Moreover, after using our modified cartridge to filter an additional 16 L of a contaminated water sample, we did not observe any marked loss in performance for the removal of As(III). Finally, our CeO_2@UiO-66@PES granules did not show signs of degradation: we did not detect any Zr(IV) or Ce(IV) in the filtered water samples in this study. Our findings demonstrate the unique functional advantages of CeO_2@UiO-66@PES granules, and we are confident that they will help bring MOF-based adsorbents one step closer to the market.

ASSOCIATED CONTENT

Supporting Information.

The supporting information is available free of charge at https://pubs.acs.org/doi/10.1021/acsami.xxxxxxx.

N_2 adsorption isotherms for the CeO_2@UiO-66 microbeads and for the CeO_2@UiO-66@PES granules with different loading values of microbeads; photographs and FE-SEM micrographs of the granules at different loading values of microbeads; a table with the BET surface areas for the CeO_2@UiO-66@PES granules with different loadings of microbeads; photograph of the adsorption set-up; a table on the removal efficiency of granules at different loading values of microbeads; XRPD and N_2 adsorption isotherm of the granules

after filtration experiments; photographs and FE-SEM micrographs of the granules after the adsorption experiments. (PDF)

AUTHOR INFORMATION

Corresponding Author

Inhar Imaz − Catalan Institute of Nanoscience and Nanotechnology (ICN2), CSIC and The Barcelona Institute of Science and Technology, 08193 Barcelona, Spain; orcid.org/ 0000-0002-0278-1141; Email: inhar.imaz@icn2.cat

Daniel Maspoch − Catalan Institute of Nanoscience and Nanotechnology (ICN2), CSIC and The Barcelona Institute of Science and Technology, 08193 Barcelona, Spain; ICREA, 08010 Barcelona, Spain; orcid.org/0000-0003-1325-9161; Email: daniel.maspoch@icn2.cat

Authors

Gerard Boix − Catalan Institute of Nanoscience and Nanotechnology (ICN2), CSIC and The Barcelona Institute of Science and Technology, 08193 Barcelona, Spain

Xu Han − Catalan Institute of Nanoscience and Nanotechnology (ICN2), CSIC and The Barcelona Institute of Science and Technology, 08193 Barcelona, Spain

Notes

The authors declare no competing financial interests.

ACKNOWLEDGMENT

This work was supported by the Spanish MINECO (project RTI2018-095622-B-I00), the Catalan AGAUR (project 2017 SGR 238), and the ERC, under the EU-FP7 (ERC-Co 615954) and Hybead 862093. It was also funded by the CERCA Program/Generalitat de Catalunya. ICN2 is supported by the Severo Ochoa program from the Spanish MINECO (Grant No. SEV-2017-0706). Xu Han thanks the China Scholarship Council (CSC) for scholarship support.

REFERENCES

(1) "Water | United Nations", https://www.un.org/en/sections/issues-depth/water/ (accessed: December, **2020**).

(2) Jaishankar, M.; Tseten, T.; Anbalagan, N.; Mathew, B. B.; Beeregowda, K. N. Toxicity, Mechanism and Health Effects of Some Heavy Metals. *Interdiscip. Toxicol*. **2014**, 7, 60–72.

(3) Gleick, P. H. Global Freshwater Resources: Soft-Path Solutions for the 21st Century. *Science* **2003**, 302, 1524–1528.

(4) Tchounwou, P. B.; Yedjou, C. G.; Patlolla, A. K.; Sutton, D. J. Heavy Metal Toxicity and the Environment. Luch A. *Molecular, Clinical and Environmental Toxicology*. Springer, Basel. **2012**, 1–30.

(5) "Secretary-General's remarks at Launch of International Decade for Action 'Water for Sustainable Development' 2018-2028 | United Nations Secretary-General", https://www.un.org/sg/en/content/sg/statement/2018-03-22/secretary-generals-remarks-launch-international-decade-action-water (accessed: December, **2020**).

(6) Pal, P. Sustainable Water-Treatment Technology. *In Industrial Water Treatment Process Technology*. Butterworth-Heinemann, Oxford. **2017**, 565–571.

(7) Adhikari, S.; Mandal, S.; Kim, D. H.; Mishra, A. K. An Overview of Treatment Technologies for the Removal of Emerging and Nanomaterials Contaminants from Municipal and Industrial Wastewater. In *Emerging and Nanomaterial Contaminants in Wastewater: Advanced Treatment Technologies*. Elsevier, Amsterdam. **2019**, 3–40.

(8) Chowdhury, S.; Mazumder, M. A. J.; Al-Attas, O.; Husain, T. Heavy Metals in Drinking Water: Occurrences, Implications, and Future Needs in Developing Countries. *Sci. Total Environ.* **2016**, 569, 476–488.

(9) Zhou, Q.; Yang, N.; Li, Y.; Ren, B.; Ding, X.; Bian, H.; Yao, X. Total Concentrations and Sources of Heavy Metal Pollution in Global River and Lake Water Bodies from 1972 to 2017. *Glob. Ecol. Conserv.* **2020**, *22*, e00925.

(10) Ridal, J.; Brownlee, B.; McKenna, G.; Levac, N. Removal of Taste and Odour Compounds by Conventional Granular Activated Carbon Filtration. *Water Qual. Res. J. Canada* **2001**, 36, 43–54.

(11) Kumar, P.; Pournara, A.; Kim, K. H.; Bansal, V.; Rapti, S.; Manos, M. J. Metal-Organic Frameworks: Challenges and Opportunities for Ion-Exchange/sorption Applications. *Prog. Mater. Sci*. **2017**, 86, 25–74.

(12) Rego, R. M.; Kuriya, G.; Kurkuri, M. D.; Kigga, M. MOF Based Engineered Materials in Water Remediation: Recent Trends. *J. Hazard. Mater.* **2021**, 403, 123605.

(13) Peng, Y.; Huang, H.; Zhang, Y.; Kang, C.; Chen, S.; Song, L.; Liu, D.; Zhong, C. A Versatile MOF-Based Trap for Heavy Metal Ion Capture and Dispersion. *Nat. Commun*. **2018**, 9, 187.

(14) Wen, J.; Fang, Y.; Zeng, G. Progress and Prospect of Adsorptive Removal of Heavy Metal Ions from Aqueous Solution Using Metal–Organic Frameworks: A Review of Studies from the Last Decade. *Chemosphere* **2018**, 201, 627–643.

(15) Li, B.; Zhang, Y.; Ma, D.; Shi, Z.; Ma, S. Mercury Nano-Trap for Effective and Efficient Removal of Mercury(II) from Aqueous Solution. *Nat. Commun.* **2014**, 5, 1–7.

(16) Mon, M.; Bruno, R.; Ferrando-Soria, J.; Armentano, D.; Pardo, E. Metal-Organic Framework Technologies for Water Remediation: Towards a Sustainable Ecosystem. *J. Mater. Chem. A* **2018**, 6, 4912–4947.

(17) Dhaka, S.; Kumar, R.; Deep, A.; Kurade, M. B.; Ji, S. W.; Jeon, B. H. Metal–Organic Frameworks (MOFs) for the Removal of Emerging Contaminants from Aquatic Environments. *Coord. Chem. Rev.* **2019**, 380, 330–352.

(18) Xia, Z.; Zhao, Y.; Darling, S. B. Covalent Organic Frameworks for Water Treatment. *Adv. Mater. Interfaces* **2021**, 8, 2001507.

(19) Fernandes, S. P. S.; Romero, V.; Espiña, B.; Salonen, L. M. Tailoring Covalent Organic Frameworks to Capture Water Contaminants. *Chem. Eur. J.* **2019**, 25, 6461–6473.

(20) Roy, D.; Neogi, S.; De, S. Adsorptive Removal of Heavy Metals from Battery Industry Effluent Using MOF Incorporated Polymeric Beads: A Combined Experimental and Modelling Approach. *J. Hazard. Mater.* **2021**, 403, 123624.

(21) Efome, J. E.; Rana, D.; Matsuura, T.; Lan, C. Q. Metal-Organic Frameworks Supported on Nanofibers to Remove Heavy Metals. *J. Mater. Chem. A* **2018**, 6, 4550–4555.

(22) Efome, J. E.; Rana, D.; Matsuura, T.; Lan, C. Q. Experiment and Modeling for Flux and Permeate Concentration of Heavy Metal Ion in Adsorptive Membrane Filtration Using a Metal-Organic Framework Incorporated Nanofibrous Membrane. *Chem. Eng. J.* **2018**, 352, 737–744.

(23) Ahmadijokani, F.; Tajahmadi, S.; Bahi, A.; Molavi, H.; Rezakazemi, M.; Ko, F.; Aminabhavi, T. M.; Arjmand, M. Ethylenediamine-Functionalized Zr-Based MOF for Efficient Removal of Heavy Metal Ions from Water. *Chemosphere* **2021**, 264, 128466.

(24) Soltani, R.; Pelalak, R.; Pishnamazi, M.; Marjani, A.; Albadarin, A. B.; Sarkar, S. M.; Shirazian, S. A Novel and Facile Green Synthesis Method to Prepare LDH/MOF Nanocomposite for Removal of Cd(II) and Pb(II). *Sci. Rep.* **2021**, 11, 1609.

(25) Du, Z.; Li, B.; Jiang, C.; Sun, R.; Chen, S. Sorption of U(VI) on Schiff-Base Functionalized Metal–organic Frameworks UiO-66-NH2. *J. Radioanal. Nucl. Chem.* **2021**, 327, 811–819.

(26) Ru, J.; Wang, X.; Wang, F.; Cui, X.; Du, X.; Lu, X. UiO Series of Metal-Organic Frameworks Composites as Advanced Sorbents for the Removal of Heavy Metal Ions: Synthesis, Applications and Adsorption Mechanism. *Ecotoxicol. Environ. Saf.* **2021**, 208, 111577.

(27) Mon, M.; Lloret, F.; Ferrando-Soria, J.; Martí-Gastaldo, C.; Armentano, D.; Pardo, E. Selective and Efficient Removal of Mercury from Aqueous Media with the Highly Flexible Arms of a BioMOF. *Angew. Chem. Int. Ed*. **2016**, 55, 11167–11172.

(28) Desai, A. V.; Manna, B.; Karmakar, A.; Sahu, A.; Ghosh, S. K. A Water-Stable Cationic Metal–Organic Framework as a Dual Adsorbent of Oxoanion Pollutants. *Angew. Chem. Int. Ed*. **2016**,7811–7815.

(29) Sun, D. T.; Peng, L.; Reeder, W. S.; Moosavi, S. M.; Tiana, D.; Britt, D. K.; Oveisi, E.; Queen, W. L. Rapid, Selective Heavy Metal Removal from Water by a Metal-Organic Framework/Polydopamine Composite. *ACS Cent. Sci.* **2018**, 4, 349–356.

(30) Feng, M.; Zhang, P.; Zhou, H. C.; Sharma, V. K. Water-Stable Metal-Organic Frameworks for Aqueous Removal of Heavy Metals and Radionuclides: A Review. *Chemosphere* **2018**, 209, 783–800.

(31) Gao, Q.; Xu, J.; Bu, X. H. Recent Advances about Metal–Organic Frameworks in the Removal of Pollutants from Wastewater. *Coord. Chem. Rev.* **2019**, 378, 17–31.

(32) From the Lab to Real-World Use. *Nat. Sustain*. **2019**, 2, 989.

(33) Boix, G.; Troyano, J.; Garzón-Tovar, L.; Camur, C.; Bermejo, N.; Yazdi, A.; Piella, J.; Bastus, N. G.; Puntes, V. F.; Imaz, I.; Maspoch, D. MOF-Beads Containing Inorganic Nanoparticles for the Simultaneous Removal of Multiple Heavy Metals from Water. *ACS Appl. Mater. Interfaces* **2020**, 12, 10554–10562.

(34) Shayegan, H.; Ali, G. A. M.; Safarifard, V. Recent Progress in the Removal of Heavy Metal Ions from Water Using Metal-Organic Frameworks. *ChemistrySelect* **2020**, 5, 124–146.

(35) Lei, C.; Gao, J.; Ren, W.; Xie, Y.; Abdalkarim, S. Y. H.; Wang, S.; Ni, Q.; Yao, J. Fabrication of Metal-Organic Frameworks@cellulose Aerogels Composite Materials for Removal of Heavy Metal Ions in Water. *Carbohydr. Polym.* **2019**, 205, 35–41.

(36) Wang, C.; Liu, X.; Chen, J. P.; Li, K. Superior Removal of Arsenic from Water with Zirconium Metal-Organic Framework UiO-66. *Sci. Rep.* **2015**, 5, 166113.

(37) Feng, Q.; Zhang, Z.; Ma, Y.; He, X.; Zhao, Y.; Chai, Z. Adsorption and Desorption Characteristics of Arsenic onto Ceria Nanoparticles. *Nanoscale Res. Lett.* **2012**, 7, 84.

(38) Recillas, S.; Colón, J.; Casals, E.; González, E.; Puntes, V.; Sánchez, A.; Font, X. Chromium VI Adsorption on Cerium Oxide Nanoparticles and Morphology Changes during the Process. *J. Hazard. Mater.* **2010**, 184, 425–431.

(39) Bux, H.; Feldhoff, A.; Cravillon, J.; Wiebcke, M.; Li, Y. S.; Caro, J. Oriented Zeolitic Imidazolate Framework-8 Membrane with Sharp H_2/C_3H_8 Molecular Sieve Separation. *Chem. Mater.* **2011**, 23, 2262–2269.

(40) Zhao, C.; Xue, J.; Ran, F.; Sun, S. Modification of Polyethersulfone Membranes - A Review of Methods. *Prog. Mater. Sci.* **2013**, 58, 76–150.

(41) Luque-Alled, J. M.; Abdel-Karim, A.; Alberto, M.; Leaper, S.; Perez-Page, M.; Huang, K.; Vijayaraghavan, A.; El-Kalliny, A. S.; Holmes, S. M.; Gorgojo, P. Polyethersulfone Membranes: From Ultrafiltration to Nanofiltration via the Incorporation of APTS Functionalized-Graphene Oxide. *Sep. Purif. Technol.* **2020**, 230, 115836.

(42) "NSF/ANSI 53-2019 - Drinking Water Treatment Units - Health Effects," can be found under https://webstore.ansi.org/Standards/NSF/NSFANSI532019?source=blog (accessed: December, **2020**).

(43) Zhang, F.; Jin, Q.; Chan, S.-W. Ceria Nanoparticles: Size, Size Distribution, and Shape. *J. Appl. Phys.* **2004**, 95, 4319–4326.

(44) Zhang, F.; Chan, S. W.; Spanier, J. E.; Apak, E.; Jin, Q.; Robinson, R. D.; Herman, I. P. Cerium Oxide Nanoparticles: Size-Selective Formation and Structure Analysis. *Appl. Phys. Lett.* **2002**, 80, 127–129.

(45) Yazdi, A.; Abo Markeb, A.; Garzón-Tovar, L.; Patarroyo, J.; Moral-Vico, J.; Alonso, A.; Sánchez, A.; Bastus, N.; Imaz, I.; Font, X.; Puntes, V.; Maspoch, D. Core-Shell Au/CeO_2 Nanoparticles Supported in UiO-66 Beads Exhibiting Full CO Conversion at 100 °C. *J. Mater. Chem. A* **2017**, 5, 13966–13970.

(46) Valizadeh, B.; Nguyen, T. N.; Smit, B.; Stylianou, K. C. Metal-Organic Framework Beads: Porous Metal-Organic Framework@Polymer Beads for Iodine Capture and Recovery Using a Gas-Sparged Column. *Adv. Funct. Mater.* **2018**, 28, 1801596.

(47) Carné-Sánchez, A.; Imaz, I.; Cano-Sarabia, M.; Maspoch, D. A Spray-Drying Strategy for Synthesis of Nanoscale Metal-Organic Frameworks and Their Assembly into Hollow Superstructures. *Nat. Chem.* **2013**, 5, 203–211.

(48) Ma, D.; Han, G.; Peh, S. B.; Chen, S. B. Water-Stable Metal-Organic Framework UiO-66 for Performance Enhancement of Forward Osmosis Membranes. *Ind. Eng. Chem. Res.* **2017**, 56, 12773–12782.

(49) Ahmadijokani, F.; Mohammadkhani, R.; Ahmadipouya, S.; Shokrgozar, A.; Rezakazemi, M.; Molavi, H.; Aminabhavi, T. M.; Arjmand, M. Superior Chemical Stability of UiO-66 Metal-Organic Frameworks (MOFs) for Selective Dye Adsorption. *Chem. Eng. J.* **2020**, 399, 125346.

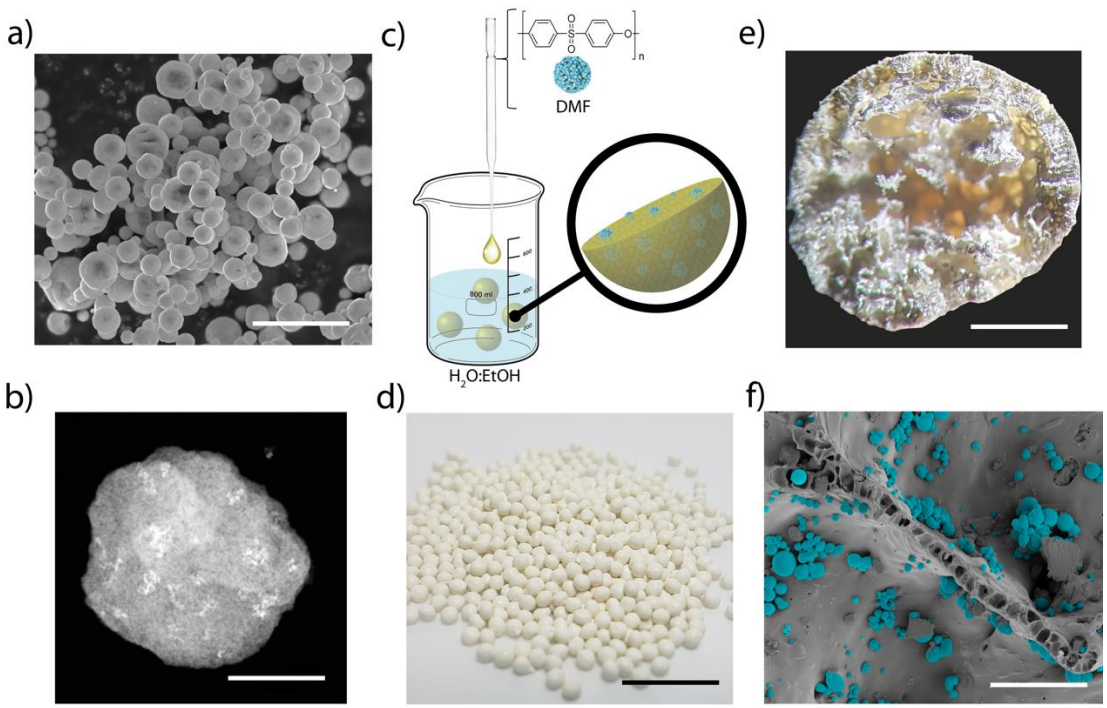

Figure 1. a) FE-SEM micrograph of spray-dried CeO_2@UiO-66 microbeads. b) HAADF-STEM micrograph of one CeO_2@UiO-66 microbead; the denser spots correspond to the CeO_2 nanoparticles. c) Schematic of the formation of CeO_2@UiO-66@PES granules via phase-inversion. d) Photograph of the synthesized millimeter-scale CeO_2@UiO-66@PES granules. e) Photograph of a cross-section of one granule. f) FE-SEM micrograph of the interior of one CeO_2@UiO-66@PES granule, at 26.1% loading of CeO_2@UiO-66 microbeads (shown in blue). Scale bars: 5 µm (a), 500 nm (b), 10 mm (d), 600 µm (e), 20 m (f).

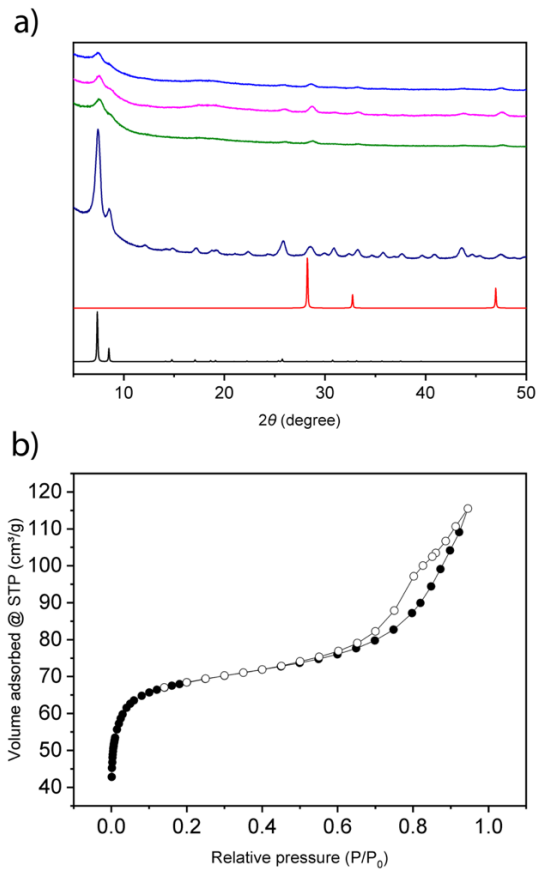

Figure 2. a) XRPD of CeO_2@UiO-66 microbeads (purple); CeO_2@UiO-66@PES granules at different microbead loading values (6.7% [blue]; 26.1% [pink], and 47.4% [green]; w/w); and the simulated peaks for UiO-66 (black) and CeO_2 nanoparticles (red). b) N_2-sorption isotherm for CeO_2@UiO-66@PES granules at a microbead loading of 26.1% (w/w).

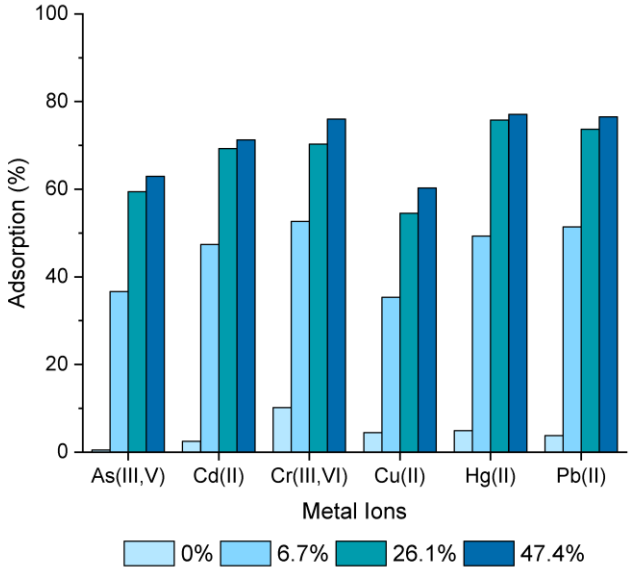

Figure 3. Adsorption performance of the PES granules loaded with CeO_2@UiO-66 microbeads at different values (w/w).

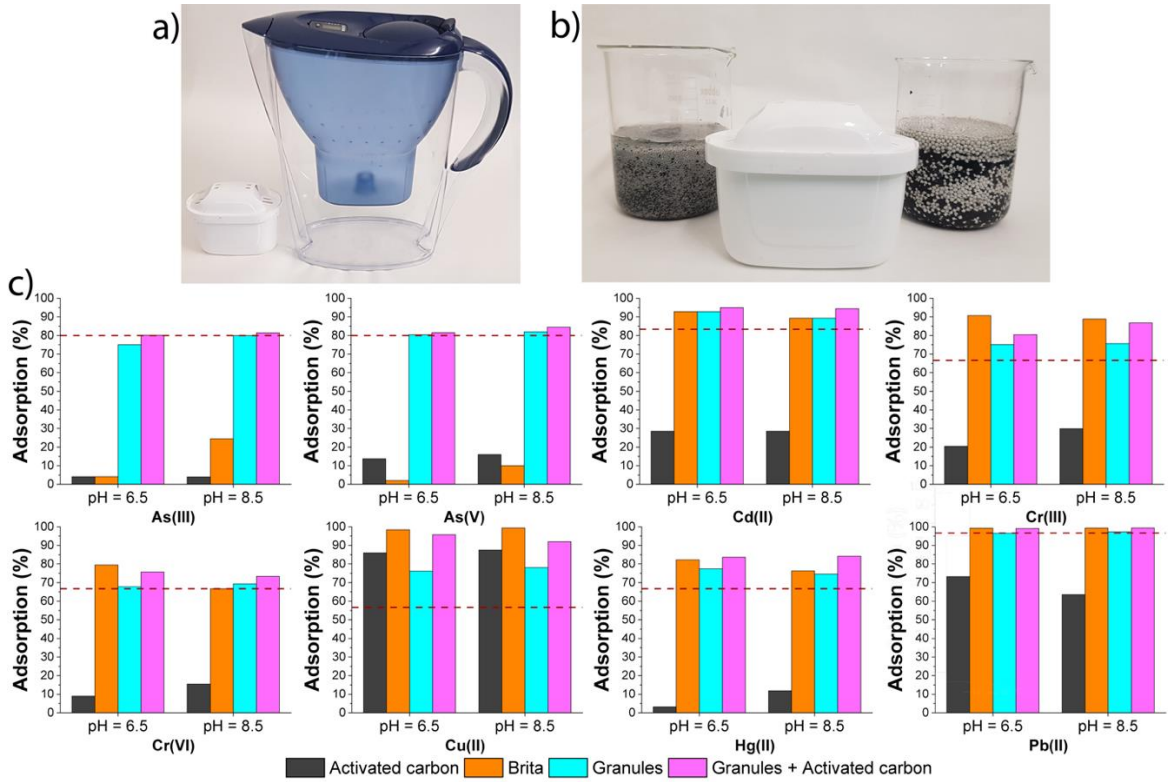

Figure 4. a) Photograph of the pitcher and cartridge used in the filtration experiments. b) Photograph of the cartridge together with the standard Brita® filter (left) and the CeO_2@UiO-66@PES granules + activated carbon filter (right). c) Adsorption performance of each cartridge at pH = 6.5 or 8.5, after filtrating 1 L of metal pollutant solution. The dashed line represents the minimum adsorption requirement to meet the NSF/ANSI standard 53-2019.

Table 1. Performance results for the four cartridges tested for removal of metals from 1 L influent solutions in a Brita® pitcher.

pH = 6.5

Metal Ion	Target Influent Concentration (ppb)	Measured Influent Concentration (ppb)	NSF/ANSI 53-2019 standard reduction target (ppb)	Activated Carbon (ppb)	Brita® (ppb)	Granules (ppb)	Granules + Activated Carbon (ppb)
As(III)	50 ± 10	49	10	46 (6%)	46 (6%)	12 (76%)	10 (80%)
As(V)	50 ± 10	51	10	44 (14%)	49 (4%)	10 (80%)	9 (82%)
Cd(II)	30 ± 7	28	5	20 (29%)	2 (93%)	2 (93%)	1 (96%)
Cr(III)	300 ± 75	293	100	233 (20%)	27 (91%)	73 (75%)	60 (80%)
Cr(VI)	300 ± 75	302	100	275 (9%)	62 (79%)	97 (68%)	75 (75%)
Cu(II)	3000 ± 750	2941	1300	412 (86%)	46 (98%)	701 (76%)	151 (95%)
Hg(II)	6 ± 1	6.2	2	5.9 (5%)	1.1 (82%)	1.4 (77%)	1.0 (84%)
Pb(II)	150 ± 15	146	5	39 (73%)	1 (99%)	5 (97%)	1 (99%)

pH = 8.5

Metal Ion	Target Influent Concentration (ppb)	Measured Influent Concentration (ppb)	NSF/ANSI 53-2019 standard reduction target (ppb)	Activated Carbon (ppb)	Brita® (ppb)	Granules (ppb)	Granules + Activated Carbon (ppb)
As(III)	50 ± 10	49	10	47 (4%)	37 (24%)	10 (80%)	9 (82%)
As(V)	50 ± 10	50	10	42 (16%)	45 (10%)	9 (82%)	8 (84%)
Cd(II)	30 ± 7	28	5	20 (29%)	3 (89%)	3 (89%)	2 (93%)
Cr(III)	300 ± 75	304	100	213 (30%)	34 (89%)	74 (76%)	41 (87%)
Cr(VI)	300 ± 75	297	100	251 (15%)	99 (67%)	91 (69%)	82 (72%)
Cu(II)	3000 ± 750	2975	1300	370 (88%)	18 (99%)	652 (78%)	250 (92%)
Hg(II)	6 ± 1	5.9	2	5.2 (12%)	1.4 (76%)	1.5 (75%)	1.0 (83%)
Pb(II)	150 ± 15	151	5	55 (64%)	1 (99%)	4 (97%)	1 (99%)

Shown are the metal-ion concentration of the influent solution, the NSF/ANSI 53-2019 standard required maximum effluent concentration, and the post-filtration effluent concentration values obtained at pH 6.5 (top) or pH 8.5 (bottom). Metal-removal values are expressed as both ppb and percentage (in parentheses).

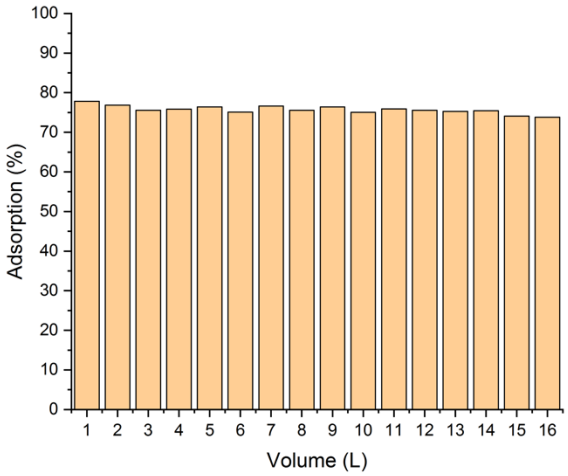

Figure 5. Performance of the cartridge containing the mixture of CeO_2@UiO-66@PES granules and activated carbon for adsorption of As(III) ions in 16 L of synthetic "hard" water containing 50 ppb As, at pH 6.5.